blood

2013 121: 2659-2668
Prepublished online February 1, 2013;
doi:10.1182/blood-2012-07-446146

Perforin forms transient pores on the target cell plasma membrane to facilitate rapid access of granzymes during killer cell attack

Jamie A. Lopez, Olivia Susanto, Misty R. Jenkins, Natalya Lukoyanova, Vivien R. Sutton, Ruby H. P. Law, Angus Johnston, Catherina H. Bird, Phillip I. Bird, James C. Whisstock, Joseph A. Trapani, Helen R. Saibil and Ilia Voskoboinik

Blood (print ISSN 0006-4971, online ISSN 1528-0020), is published weekly by the American Society of Hematology, 2021 L St, NW, Suite 900, Washington DC 20036.

Regular Article

IMMUNOBIOLOGY

Perforin forms transient pores on the target cell plasma membrane to facilitate rapid access of granzymes during killer cell attack

Jamie A. Lopez,[1-3] Olivia Susanto,[1] Misty R. Jenkins,[1-3] Natalya Lukoyanova,[4] Vivien R. Sutton,[1] Ruby H. P. Law,[5,6] Angus Johnston,[7] Catherina H. Bird,[5] Phillip I. Bird,[5] James C. Whisstock,[5,6] Joseph A. Trapani,[1,2,8] Helen R. Saibil,[4] and Ilia Voskoboinik[1-3,9]

[1]Cancer Immunology Program, Peter MacCallum Cancer Centre, East Melbourne, VIC, Australia; [2]Sir Peter MacCallum Department of Oncology and [3]Department of Pathology, University of Melbourne, Parkville, VIC, Australia; [4]Crystallography, Institute for Structural and Molecular Biology, Birkbeck College, London, United Kingdom; [5]Department of Biochemistry and Molecular Biology, Monash University, Melbourne, VIC, Australia; [6]Australian Research Council Centre of Excellence in Structural and Functional Microbial Genomics, Monash University, Clayton, VIC, Australia; and Departments of [7]Chemical and Biomolecular Engineering, [8]Microbiology and Immunology, and [9]Genetics, University of Melbourne, Parkville, VIC, Australia

Key Points

- Granzymes diffuse through perforin pores on the target cell plasma membrane.

Cytotoxic lymphocytes serve a key role in immune homeostasis by eliminating virus-infected and transformed target cells through the perforin-dependent delivery of pro-apoptotic granzymes. However, the mechanism of granzyme entry into cells remains unresolved. Using biochemical approaches combined with time-lapse microscopy of human primary cytotoxic lymphocytes engaging their respective targets, we defined the time course of perforin pore formation in the context of the physiological immune synapse. We show that, on recognition of targets, calcium influx into the lymphocyte led to perforin exocytosis and target cell permeabilization in as little as 30 seconds. Within the synaptic cleft, target cell permeabilization by perforin resulted in the rapid diffusion of extracellular milieu–derived granzymes. Repair of these pores was initiated within 20 seconds and was completed within 80 seconds, thus limiting granzyme diffusion. Remarkably, even such a short time frame was sufficient for the delivery of lethal amounts of granzymes into the target cell. Rapid initiation of apoptosis was evident from caspase-dependent target cell rounding within 2 minutes of perforin permeabilization. This study defines the final sequence of events controlling cytotoxic lymphocyte immune defense, in which perforin pores assemble on the target cell plasma membrane, ensuring efficient delivery of lethal granzymes. (*Blood*. 2013;121(14):2659-2668)

Introduction

Perforin is a pore-forming member of the membrane-attack-complex-perforin (MACPF) family of proteins.[1-3] It is stored in the secretory granules of cytotoxic lymphocytes (CLs), which seek out and bind virus-infected or transformed target cells and form a transient immunologic synapse. Upon activation by a target cell, the CL triggers the exocytosis of secretory granules containing perforin and the proapoptotic serine proteases, including granzyme B, into the synaptic cleft, resulting in target cell death.[4] Although granzyme B applied to target cells alone can be internalized through endocytosis, it remains inert and unable to reach its cytosolic substrates[5,6]; perforin's key function is thus to enable granzyme delivery into the cytosol to initiate apoptosis. Consistent with this, perforin-deficient CLs are unable to kill target cells through the granule pathway. As a result, perforin-deficient mice are unable to clear many viral infections, and this is manifested as major immune dysregulation; these mice also fail to reject transplanted tumors and develop spontaneous B-cell lymphomas as they age.[7] Humans deficient in functional perforin develop familial hemophagocytic lymphohistiocytosis (FHL),[8] and recent work suggests some individuals with incomplete loss of perforin function are predisposed to hematologic cancers.[9] Overall, perforin is essential for CL function in the immune surveillance of viral infections and cancer.

How perforin enables the delivery of granzymes into the cytosolic compartment of the target cell is a fundamentally important immunological process but has remained largely unresolved, despite significant research efforts. Our recent structural studies have definitively shown that perforin monomers polymerize to form a range of pores, the majority having internal diameters of 120 to 170 Å, which easily allows for *trans*-lumenal diffusion of granzyme molecules, typically ~50 Å in diameter.[10] A lack of direct evidence for pores of this magnitude on the target cell plasma membrane previously led scientists to hypothesize a more complex, multistep route of granzyme delivery[11-16]: rather, perforin was proposed to perturb the target cell plasma membrane by forming very small or partial pores[17] to allow the cytosolic entry of calcium ions and trigger the coendocytosis of perforin and granzyme into an endosomal compartment. Within this compartment, perforin was suggested to finally reassemble into much larger pores, allowing "leakage" of granzymes into the cytosol.

In view of our recent structural findings, we revisited perforin pore formation on the target cell plasma membrane. In the present study, we performed a detailed kinetic analysis of perforin's action on target cells using bona fide killer/target cell conjugates, as well as purified cytotoxins. Critically, we designed a novel technique to demonstrate, for the first time, the precise moment at which perforin permeabilizes

Submitted July 29, 2012; accepted January 20, 2013. Prepublished online as *Blood* First Edition paper, February 1, 2013; DOI 10.1182/blood-2012-07-446146.

The online version of this article contains a data supplement.

The publication costs of this article were defrayed in part by page charge payment. Therefore, and solely to indicate this fact, this article is hereby marked "advertisement" in accordance with 18 USC section 1734.

the target cell membrane and elicits a rapid influx of the extracellular milieu (including granzymes) into the target cell cytosol. Upon delivery of this lethal hit, target cells evoked a membrane repair response to reseal the site of perforin damage, ultimately limiting osmotic stress and cell lysis. Despite this, we found that the amount of granzyme diffusing into the cell during this short time frame (around 80 seconds) was invariably fatal for the target cell. Our current study therefore gives credence to the diffusion model as the likely mechanism through which granzymes are delivered via perforin pores at the plasma membrane to initiate apoptosis.

Methods

Isolation of primary human cytotoxic lymphocytes from peripheral blood was performed in accordance with Peter MacCallum Cancer Institute Ethics Committee Project No. 01/14. The isolation of primary mice CLs was approved by Peter MacCallum Cancer Centre Animal Ethics Committee Project No. E393.

Reagents

Compound 20 was obtained from Bespoke Medicinal Chemistry (Shanghai, China). The rat anti-human BH3 interacting-domain death agonist (Bid) antibody was a gift from R. Kluck (Walter and Eliza Hall Institute, Melbourne, Australia), and the mouse monoclonal anti-perforin antibody (P1-8) was a gift from H. Yagita (Juntendo University, Tokyo, Japan). Standard commercial reagents are described in the supplemental Materials on the *Blood* website.

Calcium flux

Jurkat cells were labeled with 2 μM Indo-1-AM for 20 minutes at 37°C/5% CO_2 in HE (150 mM NaCl, 20 mM *N*-2-hydroxyethylpiperazine-*N*'-2-ethanesulfonic acid [HEPES], 1 mM $MgCl_2$, 0.1% [w/v] bovine serum albumin [BSA]). Cells were washed twice in HE and then resuspended in RPMI 1640, 0.1% (w/v) BSA. Cells were resuspended to 1×10^5 cells/mL in RPMI 1640 media. Relative intracellular calcium concentrations were determined by the ratio of violet:blue (420:510 nm) wavelengths using the FACsVantage SE DiVa flow cytometer (BD Biosciences). Cells were maintained at 37°C, and a baseline reading was established before addition of recombinant perforin. Mean Indo-1 ratios were determined using FlowJo software.

Bid cleavage assays

HeLa cells were trypsinized, washed twice in Dulbecco's modified Eagle medium containing 0.1% (w/v) BSA and then resuspended to 1×10^6 cells/mL in Dulbecco's modified Eagle medium, 0.1% (w/v) BSA. Cells were treated with a sublytic dose of perforin (15-35 ng/mL/1×10^6 cells) and incubated at 37°C. Cell aliquots were removed and combined with media containing 62.5 nM granzyme B at various times after perforin addition. Cells were incubated for a further 10 minutes at 37°C after granzyme addition and then transferred to ice. Cells were washed twice in ice-cold phosphate-buffered saline and resuspended in lysis buffer (250 mM NaCl, 25 mM HEPES, 2.5 mM EDTA, 0.1% [v/v] NP-40, 80 μM aprotinin, 1 mM 4-(2-Aminoethyl)benzensulfonyl fluoride, 1 mM pepstatin A, 2 mM leupeptin) containing 50 μM compound (to inhibit postlysis Bid cleavage). Cells were incubated on ice for 10 minutes and centrifuged at 16 100*g*, and the supernatant was retained for Bid immunoblot analysis. Bid cleavage assays in Jurkat cells were performed as described above for the HeLa cells, except RPMI 1640 containing 0.1% (w/v) BSA media was used.

Negative stain electron microscopy

Wild-type mouse perforin (3 μL, 5-10 μg/mL) in 150 mM NaCl, 1 mM $CaCl_2$, and 50 mM L-Maleic acid, MES buffer, pH 6.0, 6.5, and 7.5, or perforin-eGFP and wild-type mouse perforin (3 μL, 10 μg/mL) in 150 mM NaCl, 1 mM $CaCl_2$, and 20 mM HEPES, pH 7.4, was incubated with PC/cholesterol (1:1 molar ratio) lipid monolayers as described previously[18] for 30 minutes at 37°C and stained with a few drops of 1% (w/v) uranyl acetate. Low-dose micrographs of negatively stained samples were recorded on a Gatan 4k×4k CCD camera (15 μm/pixel) using a Tecnai F20 microscope (FEI) at 200 keV and ×67 000 magnification. Additional information is provided in supplemental Materials.

Results

Repair of perforin pores at the plasma membrane restricts granzyme entry

To understand the mechanism of perforin-mediated granzyme delivery, we first sought to investigate the precise kinetics of perforin pore formation on the target cell plasma membrane. We studied large numbers of cells in all our assays to ensure statistically sound results. Initially, we examined the kinetics of calcium restoration using the ratiometric calcium dye Indo-1. Consistent with previous studies,[11] treatment of Jurkat cells with sublytic perforin alone (a dose resulting in <10% cell death by lysis over a 30-minute incubation period; supplemental Figure 1A) produced rapid calcium influx, with maximal levels achieved at 3 minutes (Figure 1A; supplemental Figure 1B). The decay phase (restoration to low cytosolic calcium) had a half-life of 2.69 ± 0.13 minutes. We proposed that the transient calcium influx reflected the formation of perforin pores, followed by rapid repair and restoration of basal cytosolic calcium by Ca^{2+} efflux pumps. To determine whether membrane trafficking can facilitate the restoration of intracellular calcium, Jurkat cells were treated with sublytic perforin for 3 minutes at 37°C, allowing intracellular calcium concentrations to reach their maxima. The cells were then either left at 37°C for the next 30 minutes or shifted to 4°C, so that both endocytosis and exocytosis would be blocked. As we found previously, calcium returned to near-baseline levels at 37°C but failed to do so at 4°C (supplemental Figure 1C). We postulated that the perforin pores had remained open because of the block in membrane repair. To test this possibility, cell viability was assessed by incorporation of 7-amino-actinomycin D (7-AAD). We found that ~10% of cells underwent lysis when allowed to recover at 37°C, whereas ~70% died after recovery at 4°C (supplemental Figure 1D). Increasing the osmotic stress by applying a higher dose of perforin further inhibited cell recovery (supplemental Figure 1E). These data indicate that transient perforin pores form on the majority of cells exposed to sublytic perforin and that membrane trafficking is a crucial mechanism for their repair. Also, this observation offers a simple mechanism behind the synergy of sublytic perforin and granzymes that results in apoptosis to the majority of treated cells (see below). Clearly, this is possible because most target cells have transmembrane pores formed on their cell surface.

To further examine the kinetics of repair, cells were exposed as before to sublytic perforin at 37°C, and cell aliquots were progressively moved to 4°C. Longer recovery at 37°C markedly reduced Jurkat cell death (Figure 1B), and escape from osmotic stress also correlated with cell capacity to exclude dextran (supplemental Figure 1F). Maximal cell lysis under these conditions occurred 2 to 3 minutes after perforin treatment, and escape from cell death (7-AAD exclusion phase) had a half-life of 2.87 ± 0.38 minutes. These data clearly show a time-dependent repair of pores formed at the plasma membrane.

If active membrane repair restores plasma membrane integrity, we predicted that granzyme entry into the cytosol (and cell death) would be restricted by the same mechanism. To formally test this hypothesis, cells were treated with sublytic perforin at 37°C, and granzyme B addition was progressively delayed. It has been shown that specific proteolytic cleavage of Bid by granzyme B is the

crucial first step in the death cascade for human granzyme B and occurs extremely rapidly (within 2 minutes) once granzyme B reaches the cytosol.[19] We therefore used Bid cleavage as a marker of effective granzyme delivery. We found Bid cleavage to be markedly diminished the longer that granzyme B addition was delayed (Figure 1C; supplemental Figure 1G), consistent with a short "window of opportunity" for granzyme entry, due to rapid membrane repair. Consistent with this observation, delaying granzyme B addition also resulted in the rapid loss of DNA fragmentation, a late manifestation of apoptosis (Figure 1D; supplemental Figure 1H). As predicted, delaying granzyme B addition also resulted in cell survival (Figure 1E; supplemental Figure 1I): the reduction of cell death had a half-life of 2.68 ± 0.16 minutes and corresponded almost precisely with the half-lives of calcium flux restoration and 7-AAD exclusion (Figure 1F). Thus, a 15-minute delay in adding granzyme B resulted in the complete loss of perforin/granzyme synergy. These data confirm that the repair of plasma membrane pores restricts the cytosolic diffusion of calcium ions and granzymes.

Rapid delivery of granzyme B and initiation of cell death

We next examined the timespan during which granzyme B's proteolytic activity in the cytosol was crucial to activate apoptosis. In these experiments, cells were treated simultaneously with perforin and granzyme B, followed by the addition of compound 20, a potent membrane permeable granzyme B inhibitor,[20] at later time points. Cell viability was assessed after a 24-hour incubation period (supplemental Figure 2). Early addition of compound 20 protected cells from perforin/granzyme-dependent death, but protection from cell death was lost if compound 20 was withheld for as little as 3 minutes (Figure 2A). Importantly, compound 20 treatment had no effect on cell viability, either alone or in combination with perforin. The early addition of compound 20 also blocked the proteolytic cleavage of Bid by granzyme B in a time-dependent manner (Figure 2B), but minimal Bid processing was necessary to initiate the apoptotic signal. Similarly, we also observed rapid (<2 minutes) cleavage of Bid by stopping the reaction with temperature restriction (4°C) in the absence of compound 20 quenching (data not shown), consistent with our previous work.[19] These data demonstrate that granzyme B activity during the first 3 minutes after it reaches the cytosol is sufficient for maximal cell death.

Rapid diffusion through repairable pores at the immunological synapse

Our recent structural characterization of perforin pores revealed an average lumen diameter of ~150 Å, easily large enough to accommodate the passage of granzymes (~50 Å diameter). However, direct evidence of passive diffusion into a target cell at the immunological synapse has never been produced. Indeed, some studies have even suggested that while uptake of calcium through the pores is possible,[21] they are too small to admit membrane impermeable dyes such as propidium iodide (PI).[11,22,23] Typically, the uptake of PI (and other DNA viability dyes) is only observed at the time of secondary necrosis, reflecting the final total loss of plasma membrane homeostasis.[24] However, the apparent lack of dye diffusion through perforin pores is surprising given the dimensions of the perforin pore.[10] Because the rate of diffusion through a pore is proportional to a solute's radius and concentration,[25] our ability to detect Ca^{2+}, but not PI movement through pores, may have simply reflected the fact that ≥4000-fold more Ca^{2+} than PI is expected to diffuse into the target cell using conventional experimental systems, given that Ca^{2+} (500 μM; RPMI 1640 media) has a diameter of 1 Å, whereas PI (1 μM) has a diameter of 8 Å. Consistent with free diffusion, we found that perforin-dependent uptake of both ^{32}P-dATP (6 Å diameter) and PI (8 Å) was concentration dependent, and the saturating concentration was proportional to diameter (supplemental Figure 3A-B). PI is almost invariably used at concentrations of 0.5 to 1.5 μM, as this is easily sufficient to distinguish dead cells that cumulatively bind PI in their nuclear DNA. However, at higher concentrations, PI can also be detected in the cytosol, as it also fluoresces on binding to cytosolic RNA.[26] Cells treated with sublytic doses of recombinant perforin in the presence of 1 to 10 μM PI showed minimal fluorescence (supplemental Figure 3B), but this was greatly increased when higher concentrations of PI (25-250 μM) were used. These data demonstrate that, contrary to the conclusions of previously published work, PI readily diffuses through perforin pores, but concentrations of PI higher than those traditionally used are needed to detect it.

To investigate whether similar uptake of PI can be demonstrated after the formation of a genuine immune synapse, we used primary human natural killer (NK) cells and HeLa target cells. As with previous studies,[24] significant cytoplasmic fluorescence did not occur (other than at secondary necrosis) when 1.5 μM PI was used. However, with 100 μM PI, we observed a sudden "blush" of cytosolic PI fluorescence emanating from the point of cell-cell contact (point X, Figure 3A; supplemental Movie 1). The fluorescence diffused across the cell to the distal pole (point Y) and accumulated in the nucleus over time. Importantly, when apoptosis was blocked using a combination of Bcl-2 overexpression, broad caspase inhibition (Q-VD-OPh), and a specific granzyme B inhibitor (compound 20),[20,27] uptake of PI was unaffected (supplemental Figure 3C). The cells remained adherent and intact, demonstrating that PI uptake was not a consequence of cell death but an early consequence of perforin action. Similar to NK cells, uptake of PI was also observed when synapses were formed between mouse $CD8^+$ T lymphocytes and mouse target cells (Figure 3B-C; supplemental Movie 2). Again, we observed PI emanating from the immune synapse followed by diffusion throughout the cytoplasm and ultimately nuclear labeling. To quantify fluorescence in the target cell as a function of time, we measured PI fluorescence at a point close to (proximal) or furthest from (distal) the immune synapse (Figure 3D). We observed a rapid increase in fluorescence proximally, which peaked at ~20 seconds (Figure 3E), followed by gradual equalization across the cell. The stabilization of PI fluorescence is consistent with formation of pores at the synapse, followed closely by their repair. Importantly, no change in intracellular PI fluorescence was observed in bystander cells; uptake of PI was confined to cells in contact with NK cells (Figure 3E).

Synchronizing the lethal hit

The early and invariant uptake of PI by target cells destined for cell death provided an easily observable reference point to which the subsequent events in the process of cell death could be conveniently related. For example, we measured the timespan between PI uptake and target cell rounding, which occurs as a consequence of cytoskeletal changes downstream of granzyme B delivery. Some cytoskeletal proteins are cleaved directly by granzyme B[28]; however, the total inhibition of granzyme B–mediated cell death by Bcl-2 overexpression[29] indicates that mitochondrial disruption and subsequent caspase-dependent cleavage is the dominant mechanism. Again, we studied large numbers of CL/target cell synapses. In 186 functional synapses that resulted in NK-mediated cell apoptosis, we found that target cell rounding occurred even within 2 minutes of the "PI blush," and >50% of rounding events occurred within 10 minutes (Figure 4A). In every case, early PI uptake and cell rounding were

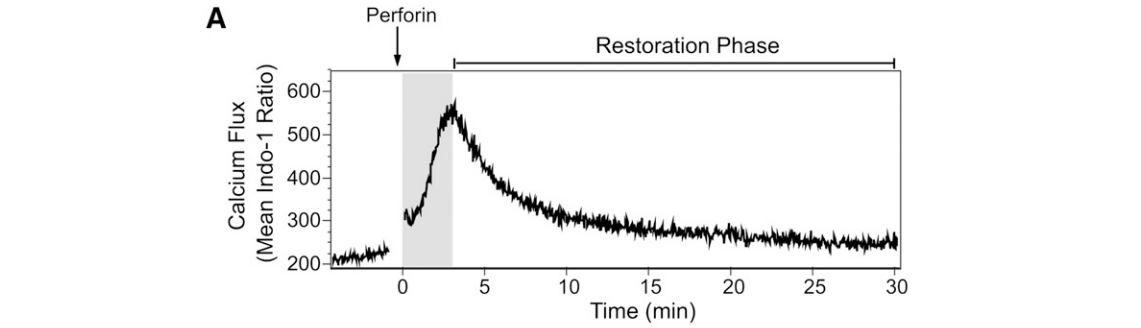

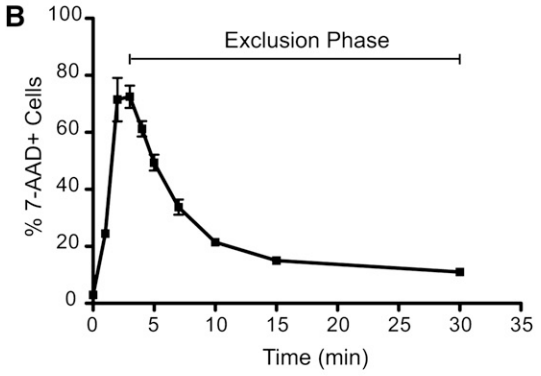

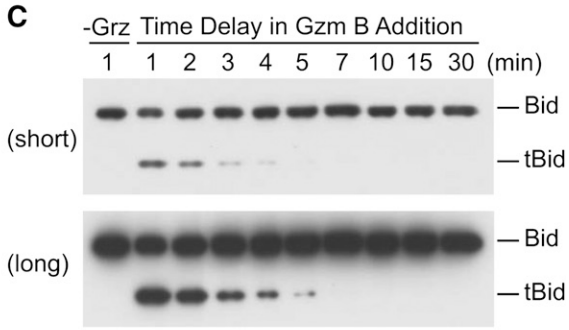

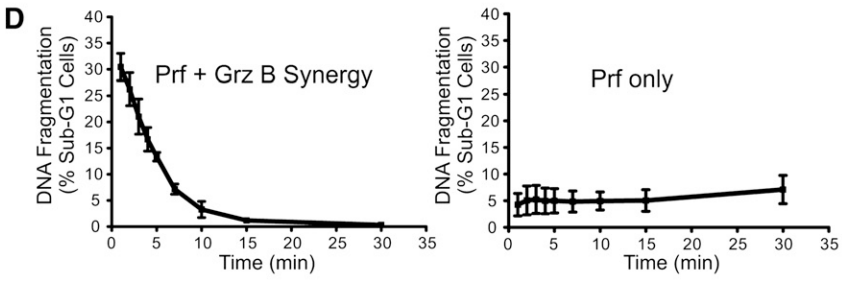

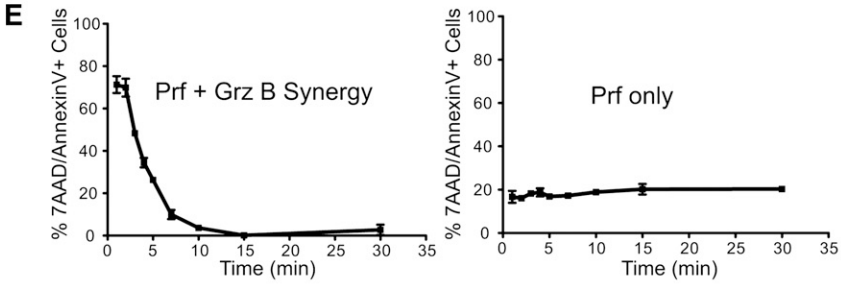

F

Parameter	$t_{1/2}$ (min)
Calcium Restoration	2.69 ± 0.13
7-AAD Exclusion	2.87 ± 0.38
Loss of Perforin and Granzyme Synergy	2.68 ± 0.16

Figure 1. Repair of perforin pores at the plasma membrane restricts granzyme delivery. Loss of diffusion through plasma membrane perforin pores inhibits target cell delivery of granzyme B. (A) Indo-1-AM–labeled Jurkat cells were treated with recombinant perforin at 37°C for 30 minutes. Relative intracellular calcium concentrations were determined by the ratio of violet:blue (420:510 nm) wavelengths. Shown are the mean Indo-1 ratio over time. Arrow indicates the addition of recombinant perforin following establishment of a baseline reading. The shaded region indicates the increase in intracellular calcium, and "Restoration Phase" represents the decrease in intracellular calcium. Data are representative of 3 independent experiments. (B) Kinetics of repair: Jurkat cells were untreated (0 minutes) or treated with perforin at 37°C before shifting cell aliquots to 4°C at 1, 2, 3, 4, 5, 7, 10, 15, or 30 minutes after perforin treatment. The percentage of 7-AAD$^+$ cells was then determined. Data represent the mean ± standard error (n = 3 independent experiments). The "Exclusion Phase" indicates the loss of 7-AAD$^+$ cells. (C) Bid cleavage analysis: Jurkat cells were treated with perforin and incubated at 37°C before shifting cell aliquots to media alone (−Grz) or media containing granzyme B (62.5 nM) at 1, 2, 3, 4, 5, 7, 10, 15, and 30 minutes after perforin

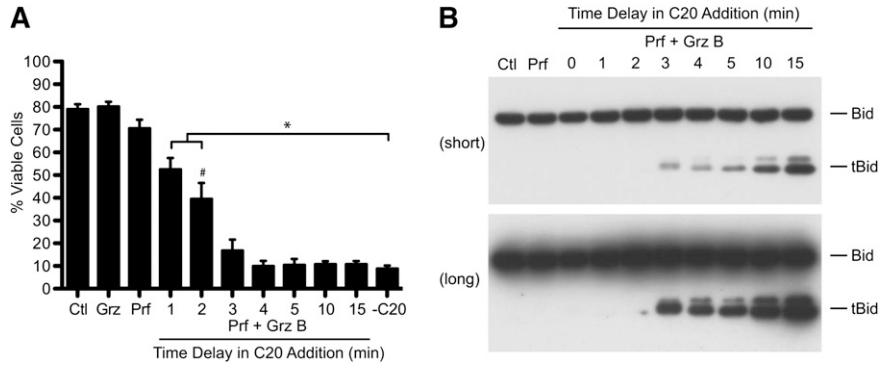

Figure 2. Rapid delivery of granzyme B and initiation of cell death. Minimal cleavage of Bid by Granzyme B is sufficient for transmission of the cell death signal. (A-B) Granzyme B activity quenching: Jurkat cells were simultaneously treated with perforin and granzyme B (62.5 nM) before shifting cell aliquots to media containing 10 μM compound 20 at 1, 2, 3, 4, 5, 10, or 15 minutes after perforin and granzyme addition. Control treatments included nontreated cells (Ctl) and granzyme B–only (Grz) or perforin-only (Prf) treatments. Cells were then either (B) incubated for a further 10 minutes at 37°C, whole cell lysates were prepared, and the formation of tBid was assessed by Bid immunoblot analysis (top, short exposure; bottom, long exposure) or (A) incubated for 24 hours at 37°C/5% CO_2 and cell viability was assessed. Data represent the mean ± standard error (n = 3 independent experiments). *$P < .05$, one-way ANOVA, Tukey post hoc test by comparison with no compound 20 (−C20) treatment; #$P < .05$, one-way ANOVA, Tukey post hoc test by comparison with perforin-only (Prf) treatment (all treatments from 2 minutes onward were significantly different to Prf). See also supplemental Figure 2.

a prelude to apoptosis. As with Bid cleavage (Figure 2), these data demonstrate the rapid delivery of granzymes during CL attack.

Conjugation of NK cells with their targets results in receptor activation and calcium influx in the killer cell. To further validate our findings, we asked whether effector cell activation preceded PI uptake in the target cells. Entry of extracellular calcium into the killer cell is essential for NK cell degranulation,[30] so we monitored intracellular calcium by labeling the human NK cells with the calcium-sensitive dye Fluo-4. Conjugate formation resulted in an increase in intracellular calcium in the effector cell that was followed, within 30 seconds to 3 minutes, by PI uptake in the target cell (Figure 4B; supplemental Movie 3). Similar findings were observed in *wt* mouse NK cells (Figure 4C; supplemental Movie 4), but as death was perforin dependent, and no PI uptake occurred if $Prf^{-/-}$ NK cells were used, despite normal conjugate formation and activation, as assessed by calcium influx (Figure 4D; supplemental Movie 5).

Endocytosis is not required for perforin- and granzyme-induced cell death

Our data to date were consistent with rapid and unidirectional granzyme entry into the target cell by direct diffusion at the plasma membrane. To explore the endosomolytic idea in detail, we generated an active recombinant perforin-eGFP reporter protein (supplemental Figure 4A-E; supplemental Materials) to visualize perforin binding to the target cell and monitor its fate directly and in real time. Using the perforin-eGFP reporter and applying 2 separate quantitative flow cytometry–based techniques, we assessed whether perforin-eGFP molecules are endocytosed following plasma membrane binding (supplemental Figure 5A-I; supplemental Materials). Our data demonstrated that perforin molecules can be internalized over time, but at the rate that was identical to the constitutive membrane recycling (supplemental Figure 5A-I).

Previous studies have shown that cells respond to pore-forming proteins such as streptolysin O by upregulating endocytosis,[31] prompting the hypothesis that endocytosis-mediated repair stimulates perforin and granzyme entry into the endosome.[11] We tested whether exposure of cells to perforin upregulated endocytosis by assessing uptake of both transferrin and wheat germ agglutinin (WGA). As shown in supplemental Figure 5J-L, perforin treatment had no significant effect on uptake of transferrin or WGA, indicating that perforin does not influence plasma membrane endocytosis.

The leaky endosome model[12,15,16] also proposes that assembly of granzyme-permeable perforin pores only occurs after endocytosis. To further determine whether endocytosis is essential for cytotoxicity, we used a number of approaches to disrupt the endocytic and intracellular trafficking pathways and then assessed granzyme B cytotoxicity. Treatment with the sterol-chelator methyl-β cyclodextrin (supplemental Figure 6A-D; supplemental Materials) or overexpression of a dominant negative dynamin K44A mutant (supplemental Figure 6E-G; supplemental Materials), which disrupt endosomal trafficking, or treatment with the microtubule depolarizing agent nocodazole (supplemental Figure 6H), had no significant inhibitory effect on perforin/granzyme cytotoxicity.

Finally, we investigated whether the acidic conditions of the endosomal compartment can support the assembly of functional pores. The early endosomal pH is generally in the range 6.0 to 6.5.[32] We examined perforin's ability both to form pores and lyse cells under various pH conditions. Consistent with previous studies,[33] perforin lysis was strongly inhibited under acid conditions with complete inactivity at pH 6.1 (data not shown). This was not caused by loss of perforin binding, consistent with previous studies.[34] Importantly, perforin was not denatured at mildly acidic pH, as its activity was

Figure 1 (continued) incubation, and then incubating for a further 10 minutes at 37°C. Whole cell lysates were prepared, and the formation of tBid was assessed by Bid immunoblot analysis. The migration of uncleaved Bid and truncated Bid (tBid) is marked on the right side of the panels. The top panel represents a short exposure, and the bottom panel is a long exposure from the same blot. Data are representative of 2 independent experiments. (D) Nuclear fragmentation (% PI+ sub-G1 nuclei): cells were treated with perforin and incubated at 37°C before shifting cell aliquots to media alone (Prf only) or media containing granzyme B (+GrzB; 15.6 nM) at 1, 2, 3, 4, 5, 7, 10, 15, and 30 minutes after perforin incubation, followed by incubation at 37°C/5% CO_2 for 3 hours. Shown is the quantification for perforin and granzyme B synergy or perforin-only treatments. Data represent the mean ± standard error (n = 3 independent experiments). (E) Phosphatidylserine exposure/7-AAD positivity: experiments were performed as in panel B, except the population of percentage of 7-AAD$^+$ and/or AnnexinV$^+$ cells was gated. Shown are the quantification for perforin and granzyme B synergy or perforin-only treatments. Data represent the mean ± standard error (n = 3 independent experiments). (F) Table shows the half-life ($t1/2$) of calcium restoration, 7-AAD exclusion (loss of 7-AAD$^+$ cells), and perforin and granzyme synergy (loss of AnnexinV$^+$ and/or 7-AAD$^+$ cells) from their maxima. Data represent the mean ± standard error (n = 3 independent experiments).

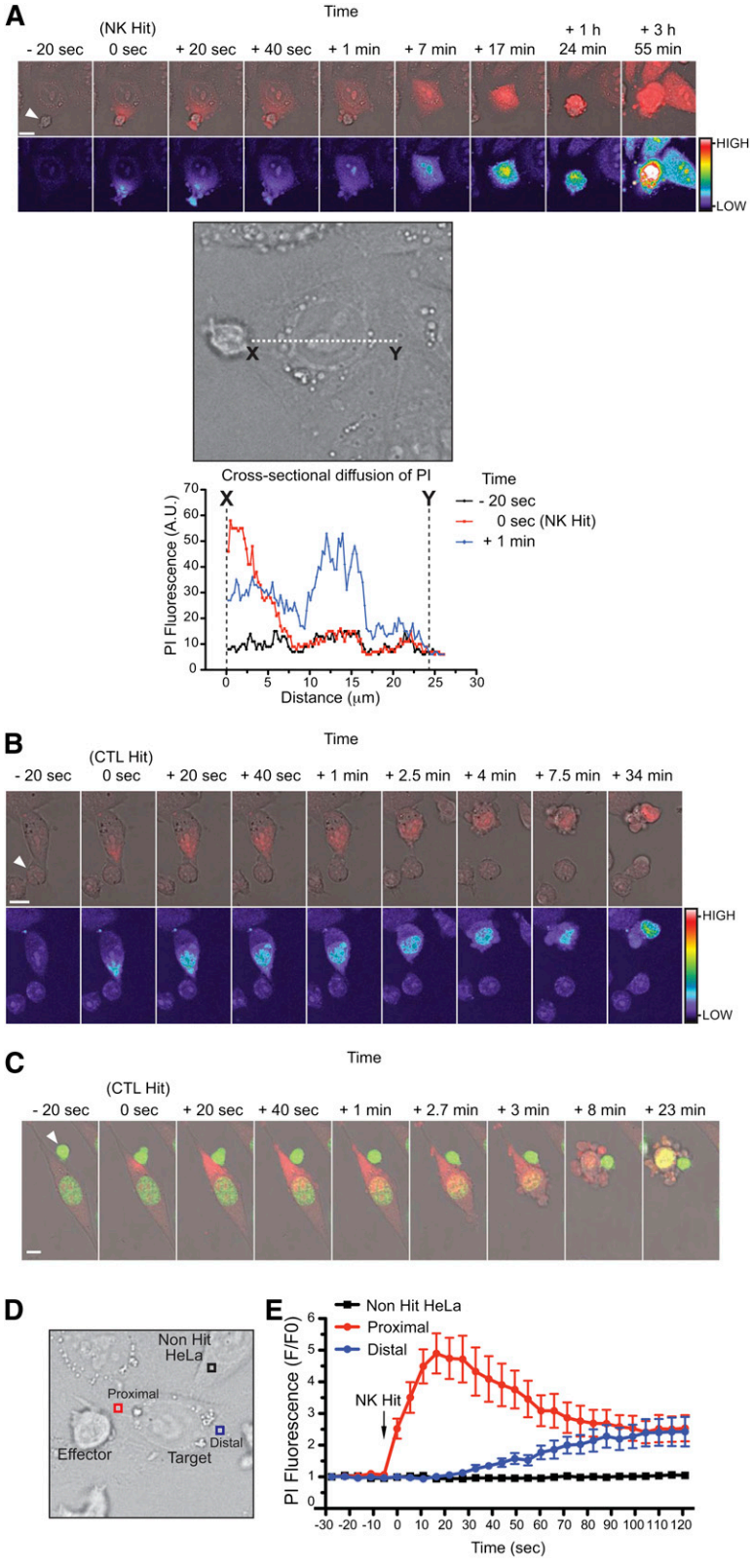

Figure 3. Rapid diffusion through repairable pores at the immunological synapse. CL-mediated diffusion of dyes into target cells at the immunological synapse. (A) Time-lapse microscopy of primary human NK cells with HeLa target cells in the presence of 100 μM PI. Images were acquired every 20 seconds and show PI(red)/Brightfield overlay (top) and PI pseudocolor (bottom; color bar indicates the pixel intensity). White arrow indicates the NK effector cell. Images depict cytosolic diffusion of PI into the target cell from the point of NK contact (0 seconds), followed by uniform cytosolic dispersion of PI (40 seconds), cell rounding (7 minutes), membrane blebbing (1 hour, 24 minutes), and secondary necrosis (3 hours, 55 minutes). Scale bar, 10 μm. Cross-sectional line scan analysis: graph shows the cross-sectional diffusion of PI fluorescence (pixel intensity) at different times from the site of NK contact (point X) to the distal point of the target cell (point Y). Cell image from the top panels has been rotated for presentation purposes. Images are representative of 5 to 10 cells from each of 5 independent experiments (using 5 different human donors). See also supplemental Movie 1. (B) Time-lapse microscopy of mouse OT-I cytotoxic T-lymphocytes and MC57-OVA257 targets in the presence of 100 μM PI. Images were acquired every 20 seconds and show PI(red)/Brightfield overlay (top) and PI pseudocolor (bottom; color bar indicates the pixel intensity). White arrow indicates the CTL effector cell. Images depict cytosolic diffusion of PI into the target from the point of CTL contact (0 seconds), followed by cytosolic dispersion of PI (40 seconds), cell rounding (2.5 minutes), membrane blebbing (4 minutes), and late stages of cell death (34 minutes). Scale bar, 10 μm. Images are representative of 5 to 10 cells from each of 5 independent experiments. (C) Time-lapse microscopy of mouse a OT-I cytotoxic T-lymphocyte and a SIINFEKL-pulsed MC57 target in the presence of 100 μM PI and 2.5 μM SYTO 24 green nuclear dye. Images were acquired every 20 seconds and show the SYTO-green(green)/PI (red)/Brightfield overlay. White arrow indicates the CTL effector cell. Images depict cytosolic diffusion of PI into the target from the point of CTL contact (0 seconds), followed by cytosolic dispersion of PI (20 seconds), cell rounding (2.7-3 minutes), membrane blebbing (8 minutes), and late stages of death (23 minutes). Scale bar, 10 μm. Images are representative of 5 to 10 cells from 2 independent experiments. See also supplemental Movie 2. (D-E) Monitoring the PI fluorescence change over time in bystander (non-hit HeLa) and target cells proximal and distal to the point of NK conjugation. Images were acquired every 5.5 seconds. Data represent the mean ± standard error for fold change (F/F0) in PI fluorescence over time (n = 12 target cells and n = 12 non-hit HeLa cells).

completely recovered when the pH was restored to 7.4 (supplemental Figure 7A). We postulated that the pH dependence of perforin activity might reflect conformational rigidity under acid conditions that would preclude pore formation. We measured the unfolding transition temperature of perforin as a function of pH via fluorescence-based thermal shift assay.[35] A decrease in pH resulted in an increase in the unfolding transition temperature, both in the absence and presence of calcium (supplemental Figure 7B). These results suggested that at low pH perforin was structurally more stable, and therefore it was energetically less favorable to undergo the conformational changes required for oligomerization and membrane insertion. To test this directly, we visualized perforin pores on lipid

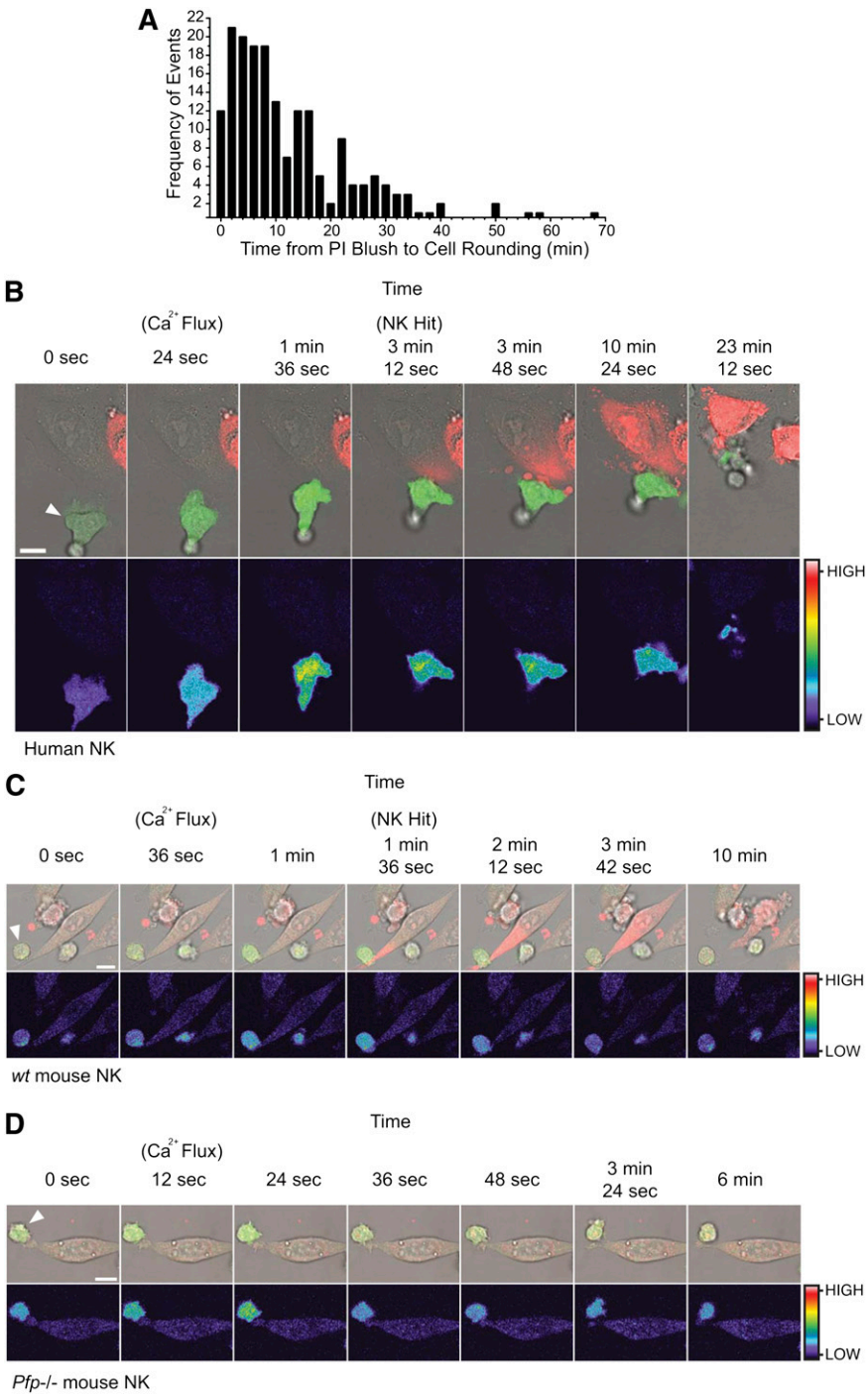

Figure 4. The synchronization of effector cell activation and target cell rounding relative to target cell PI uptake. Target cells rapidly round following uptake of PI. (A) Frequency distribution of the times (minutes) between the PI blush to the first sign of cell rounding. Columns represent 2-minute time intervals (n = 186 apoptotic target cell deaths from 3 independent human donors). Effector cell activation precedes target cell PI uptake. (B) Time-lapse microscopy of 1 μM Fluo-4-AM–labeled human NK cells with HeLa target cells. Images depict an increase in NK Fluo-4 fluorescence on attachment to the HeLa target (24 seconds), prior to PI uptake by the target (3 minutes, 12 seconds), and subsequent detachment of the effector cell (23 minutes, 12 seconds). Images are representative of 5 to 10 cells from 6 independent experiments (using 6 different human donors). See also supplemental Movie S3. (C) Time-lapse microscopy of 1 μM Fluo-4-AM–labeled *wt* mouse NK cell with a MC57 target cell showing an increase in NK Fluo-4 fluorescence on attachment to the MC57 target (36 seconds to 1 minute) and prior to PI uptake by the target (1 minute, 36 seconds). Images are representative of 5 to 10 cells from 3 independent experiments. See also supplemental Movie S4. (D) Time-lapse microscopy of 1 μM Fluo-4-AM–labeled $pfp^{-/-}$ mouse NK cell with a MC57 target cell showing an increase in NK Fluo-4 fluorescence on attachment to the MC57 target (12-24 seconds) but no subsequent PI uptake. Images are representative of 5 to 10 cells from 3 independent experiments. See also supplemental Movie S5. All images (B-D) were acquired every 12 seconds and show Fluo-4(green)/PI(red)/Brightfield overlay (top) and Fluo-4 pseudocolor (bottom; color bar indicates the pixel intensity). White arrows indicate the NK effector cell. Scale bars, 10 μm.

monolayers by negative stain electron microscopy (EM). Although pores were readily seen at neutral pH, few were formed at pH 6.5 and none at pH 6.0, despite the protein being able to bind to the monolayer (Figure 5). The acidic environment of the endosome is therefore incompatible with formation of perforin pores. Even when the endosomal compartment was deacidified with the highly specific vacuolar proton pump inhibitor bafilomycin A1,[36] no effect on perforin-dependent granzyme B cytotoxicity was observed (supplemental Figure 7C), consistent with the pores having already formed on the cell surface.

Although we cannot completely eliminate the possibility that some granzyme may enter by other mechanisms, our data demonstrate that endocytosis is unlikely to play a dominant role in perforin-mediated granzyme delivery.

Discussion

In this study, we elucidated the functional mechanism of perforin-mediated granzyme delivery during CL attack. Our results demonstrate that perforin forms transient pores on the surface of target cells, providing a short window of time for direct entry of granzymes into the cytosol.

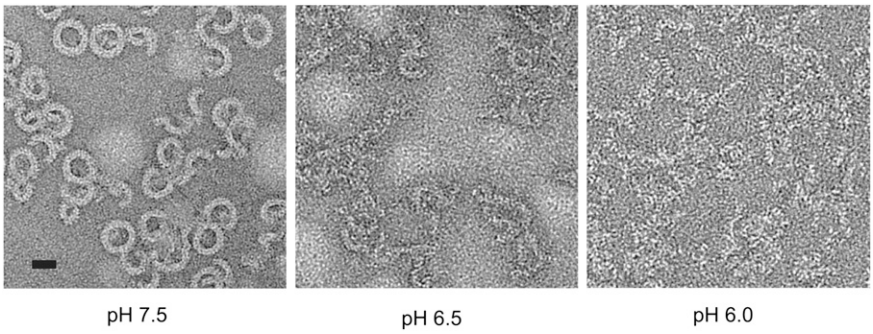

Figure 5. Perforin oligomerization is pH dependent. pH-dependent perforin pore formation. Negative stain EM images of perforin oligomers formed at pH 6.0, 6.5 and 7.5 on lipid monolayers. Scale bar, 20 nm.

Early observations in the 1980s[1,2] clearly showed that perforin forms large (150 Å) transmembrane pores. However, because of the inability to measure diffusion of granzymes through these pores and the lack of knowledge on perforin structure, the field sought alternative explanations for perforin and granzyme synergy: the endosomolysis mechanism. According to this hypothesis, perforin forms small granzyme-impermeable pores on the target membrane, which facilitate perforin and granzyme entry through cointernalization. Importantly, one of the most compelling pieces of evidence against diffusion of granzymes through plasma membrane pores was that previous studies examining the action of sublytic perforin on cells have not revealed the uptake of relatively small (eg, PI, ~8 Å) fluorescent dyes by target cells,[11,22,37] despite efficient uptake of smaller (~1 Å) Ca^{2+} ions. Indeed, our own previous studies suggested perforin pores formed on the plasma membrane were too small to allow diffusion of membrane impermeable dyes because when conventional concentrations of the membrane impermeable dye PI (0.5-1.5 μM) were used, PI staining was only observed in cells late in apoptosis, when significant accumulation of PI had occurred in DNA.[24,27]

We recently demonstrated by cryo-EM analyses that the dimensions of the perforin pore (150-200 Å) are easily large enough to accommodate the passage of granzymes (~50 Å) and, by default, smaller nuclear dyes. These new structural insights led us to revisit the mechanism by which CLs use the pore-forming perforin to deliver granzymes. We refined experimental systems so that they would be capable of detecting transmembrane diffusion and demonstrated that earlier experimental approaches did not resolve the time point at which the membrane is breached by perforin pores. Indeed, our new experimental conditions revealed the following: (1) the precise timing of effector cell activation (Ca^{2+} influx), followed by (2) perforin-dependent membrane disruption (PI influx within ~3 minutes), (3) membrane resealing (initiated within 20 seconds, with complete stabilization of intracellular PI by 80 seconds), and (4) remarkably rapid initiation of apoptosis (>50% cells underwent rounding within 10 minutes). This sequence of events has never been resolved and measured in the past. Overall, the apparent consistency between our in vitro data using recombinant reagents and measurements under physiological immune synapse conditions provides direct and compelling evidence for the formation of granzyme-permeable pores on the target cell plasma membrane. Furthermore, the "blush" of PI fluorescence revealed in the current study offers a unique and useful tool that marks delivery of the lethal hit by perforin-dependent killer cells, which will be valuable for future studies investigating the cytotoxic immune synapse.

Membrane repair of perforin pores has been previously described by others[11] and resembles the membrane repair response observed following treatment of cells with bacterial pore-forming streptolysin O.[38,39] However, unlike previous studies with perforin,[11,13] our experiments have directly demonstrated using a variety of experimental strategies that the repair of perforin pores from the cell surface does not facilitate entry of granzyme B into the cytosolic compartment but rather precludes it. This leaves only a very short window of opportunity for granzyme B delivery into the cytosol, which is nevertheless sufficient for processing a lethal amount of Bid. Using various readouts of perforin-induced membrane damage, the time of repair remained remarkably predictive of the loss of perforin and granzyme synergy, further validating our conclusions. These data highlight the essential requirement for the near-synchronous delivery of both perforin and granzyme B. An unexpected but fascinating offshoot of these studies was providing the explanation for a phenomenon that has puzzled the field for a long time: how nontoxic concentrations of perforin allow delivery of granzyme B, causing death to almost every cell exposed. We showed that even sublytic amounts of perforin are sufficient to allow the formation of pores capable of transiting granzyme B into most cells in the population; however, these cells can rapidly repair the damage and thus resist lysis. This is in contrast to earlier findings that suggested sublytic perforin only acts on a subset of cells within the population, prompting the conclusion that granzymes could enter target cells even in the absence of detectable plasma membrane pore formation.[22]

Perforin and granzyme molecules can be endocytosed from the target cell surface over time, as does any other extracellular material. Indeed in our study, we generated functional fluorescent perforin and directly measured its rate of uptake in live cells. Uptake of perforin was indistinguishable from constitutive membrane internalization (WGA uptake). Similarly, constitutive uptake of granzyme B into the endosomal compartment is well documented, yet it remains inert within these compartments.[5,6,40,41] Consistent with this, endocytosis of perforin and granzymes was not required for cell death, because disruption of key mediators of endocytosis and intracellular trafficking including dynamin-dependent endocytosis, cholesterol-dependent endosomal trafficking, or microtubule integrity, had no effect on granzyme B cytotoxicity. This is in agreement with previous studies, where overexpression of dominant negative rab5 and knockdown of key players of the clathrin-dependent endocytosis pathway had no significant effect on the capacity of CLs to induce target cell death.[13,32,42]

Our data suggest that diffusion of granzymes through transmembrane perforin pores appears to be the dominant mechanism of granzyme delivery to the target. However, we cannot completely exclude the possibility that incomplete pores or "arcs" proposed by Praper et al[17] may trigger a slower, albeit concurrent, endocytic granzyme delivery pathway.

Clearly, one of the keys to perforin's mode of action appears to be its dependence on the neutral pH and high Ca^{2+} found within the extracellular environment, whereas acidification and calcium depletion associated with endocytic compartments[43] are incompatible with perforin pore formation. Therefore, although perforin binding to lipid membranes is likely to be a stochastic, Ca^{2+}-dependent process,

our direct cryo-EM analysis demonstrated that the pH of the membrane environment controls its capacity for oligomerization and pore formation.

The current findings also led us to revisit our previous work in which we were unable to visualize passage across the target cell plasma membrane of fluorescein isothiocyanate (FITC)-labeled granzyme B delivered with sublytic perforin, which then caused us to propose a role for perforin in endosomal disruption.[16] The concentration of granzyme B used in the 1999 study was typically 25 to 75 nM, as this amount potently induces cell death. Given that visualizing diffusion of PI through perforin pores in the current study required PI concentrations around 100-fold higher, it is hardly surprising, in retrospect, that our study and several other subsequent ones were not able to directly show FITC-granzyme B in the cytosol. Ironically, our 1999 study used nuclear accumulation of FITC-granzyme B as a late marker of target cell death: granzyme B, a very basic (theoretical pI > 9.0) cationic molecule, has strong ionic affinity for anionic DNA. It is only when FITC-granzyme B becomes strongly concentrated that it, like PI, can be readily detected by light microscopy.

In conclusion, this study has resolved one of the critical mechanisms of the immune defense: the delivery of the lethal hit by CLs. Using an evolutionarily conserved mechanism of oligomerization and pore formation, the key effector molecule perforin has evolved to function within the high calcium and neutral pH conditions found within the extracellular environment of the immune synapse. We showed that delivery of the lethal hit at the immunological synapse occurs through transient perforin pore formation on the plasma membrane surface of target cells. This provides a direct and most efficient means of delivering the lethal granzyme cargo. This process represents a rate-limiting step used by the innate and adaptive arms of the immune response to eliminate virus-infected and transformed cells within the body.

Acknowledgments

The authors thank Mark Smyth and Amelia Brennan for critical reading of the manuscript; Ralph Rossi, Sarah Ellis, and Jesse Rudd-Schmidt for technical assistance; and Sandra Verschoor and Annette Ciccone for preparation of recombinant perforin protein.

J.A.L. is supported by a National Health and Medical Research Council (NHMRC) postdoctoral training fellowship. O.S. is supported by a Cancer Research Institute predoctoral tumor immunology scholarship. M.R.J. is supported by an NHMRC/R.G. Menzies postdoctoral training fellowship. I.V., J.A.T., P.I.B., and J.C.W. are supported by fellowships and grants from the NHMRC. J.C.W. is an Australian Research Council Federation Fellow. H.R.S. thanks the Wellcome Trust and the UK Biotechnology and Biological Sciences Research Council for support.

Authorship

Contribution: J.A.L. and I.V. designed and performed the experiments, analyzed the data, and wrote the paper. O.S., M.R.J., C.H.B., N.L., V.R.S., R.H.P.L., and A.J. designed and/or performed experiments and analyzed the data. H.R.S., J.C.W., P.I.B., and J.A.T. helped design the experiments and wrote the paper.

Conflict-of-interest disclosure: The authors declare no competing financial interests.

Correspondence: Ilia Voskoboinik, Cancer Immunology Program, Peter MacCallum Cancer Centre, St. Andrews Place, East Melbourne, VIC 3002, Australia; e-mail: ilia.voskoboinik@petermac.org.

References

1. Podack ER, Dennert G. Assembly of two types of tubules with putative cytolytic function by cloned natural killer cells. *Nature.* 1983;302(5907):442-445.
2. Dourmashkin RR, Deteix P, Simone CB, et al. Electron microscopic demonstration of lesions in target cell membranes associated with antibody-dependent cellular cytotoxicity. *Clin Exp Immunol.* 1980;42(3):554-560.
3. Shinkai Y, Takio K, Okumura K. Homology of perforin to the ninth component of complement (C9). *Nature.* 1988;334(6182):525-527.
4. de Saint Basile G, Ménasché G, Fischer A. Molecular mechanisms of biogenesis and exocytosis of cytotoxic granules. *Nat Rev Immunol.* 2010;10(8):568-579.
5. Shi L, Mai S, Israels S, et al. Granzyme B (GraB) autonomously crosses the cell membrane and perforin initiates apoptosis and GraB nuclear localization. *J Exp Med.* 1997;185(5):855-866.
6. Bird CH, Sun J, Ung K, et al. Cationic sites on granzyme B contribute to cytotoxicity by promoting its uptake into target cells. *Mol Cell Biol.* 2005;25(17):7854-7867.
7. Trapani JA, Smyth MJ. Functional significance of the perforin/granzyme cell death pathway. *Nat Rev Immunol.* 2002;2(10):735-747.
8. Stepp SE, Dufourcq-Lagelouse R, Le Deist F, et al. Perforin gene defects in familial hemophagocytic lymphohistiocytosis. *Science.* 1999;286(5446):1957-1959.
9. Chia J, Yeo KP, Whisstock JC, et al. Temperature sensitivity of human perforin mutants unmasks subtotal loss of cytotoxicity, delayed FHL, and a predisposition to cancer. *Proc Natl Acad Sci USA.* 2009;106(24):9809-9814.
10. Law RHP, Lukoyanova N, Voskoboinik I, et al. The structural basis for membrane binding and pore formation by lymphocyte perforin. *Nature.* 2010;468(7322):447-451.
11. Keefe D, Shi L, Feske S, et al. Perforin triggers a plasma membrane-repair response that facilitates CTL induction of apoptosis. *Immunity.* 2005;23(3):249-262.
12. Thiery J, Keefe D, Boulant S, et al. Perforin pores in the endosomal membrane trigger the release of endocytosed granzyme B into the cytosol of target cells. *Nat Immunol.* 2011;12(8):770-777.
13. Thiery J, Keefe D, Saffarian S, et al. Perforin activates clathrin- and dynamin-dependent endocytosis, which is required for plasma membrane repair and delivery of granzyme B for granzyme-mediated apoptosis. *Blood.* 2010;115(8):1582-1593.
14. Praper T, Sonnen AF-P, Kladnik A, et al. Perforin activity at membranes leads to invaginations and vesicle formation. *Proc Natl Acad Sci USA.* 2011;108(52):21016-21021.
15. Froelich CJ, Orth K, Turbov J, et al. New paradigm for lymphocyte granule-mediated cytotoxicity. Target cells bind and internalize granzyme B, but an endosomolytic agent is necessary for cytosolic delivery and subsequent apoptosis. *J Biol Chem.* 1996;271(46):29073-29079.
16. Browne KA, Blink E, Sutton VR, et al. Cytosolic delivery of granzyme B by bacterial toxins: evidence that endosomal disruption, in addition to transmembrane pore formation, is an important function of perforin. *Mol Cell Biol.* 1999;19(12):8604-8615.
17. Praper T, Sonnen A, Viero G, et al. Human perforin employs different avenues to damage membranes. *J Biol Chem.* 2011;286(4):2946-2955.
18. Dang TX, Hotze EM, Rouiller I, et al. Prepore to pore transition of a cholesterol-dependent cytolysin visualized by electron microscopy. *J Struct Biol.* 2005;150(1):100-108.
19. Sutton VR, Davis JE, Cancilla M, et al. Initiation of apoptosis by granzyme B requires direct cleavage of bid, but not direct granzyme B-mediated caspase activation. *J Exp Med.* 2000;192(10):1403-1414.
20. Willoughby CA, Bull HG, Garcia-Calvo M, et al. Discovery of potent, selective human granzyme B inhibitors that inhibit CTL mediated apoptosis. *Bioorg Med Chem Lett.* 2002;12(16):2197-2200.
21. Poenie M, Tsien RY, Schmitt-Verhulst AM. Sequential activation and lethal hit measured by [Ca2+]i in individual cytolytic T cells and targets. *EMBO J.* 1987;6(8):2223-2232.
22. Metkar SS, Wang B, Aguilar-Santelises M, et al. Cytotoxic cell granule-mediated apoptosis: perforin delivers granzyme B-serglycin complexes into target cells without plasma membrane pore formation. *Immunity.* 2002;16(3):417-428.
23. Metkar SS, Wang B, Catalan E, et al. Perforin rapidly induces plasma membrane phospholipid flip-flop. *PLoS ONE.* 2011;6(9):e24286.
24. Waterhouse NJ, Sutton VR, Sedelies KA, et al. Cytotoxic T lymphocyte-induced killing in the

absence of granzymes A and B is unique and distinct from both apoptosis and perforin-dependent lysis. *J Cell Biol.* 2006;173(1):133-144.

25. Renkin EM. Filtration, diffusion, and molecular sieving through porous cellulose membranes. *J Gen Physiol.* 1954;38(2):225-243.
26. Rieger AM, Hall BE, Luong T, et al. Conventional apoptosis assays using propidium iodide generate a significant number of false positives that prevent accurate assessment of cell death. *J Immunol Methods.* 2010;358(1-2):81-92.
27. Sedelies KA, Ciccone A, Clarke CJP, et al. Blocking granule-mediated death by primary human NK cells requires both protection of mitochondria and inhibition of caspase activity. *Cell Death Differ.* 2008;15(4):708-717.
28. Browne KA, Johnstone RW, Jans DA, et al. Filamin (280-kDa actin-binding protein) is a caspase substrate and is also cleaved directly by the cytotoxic T lymphocyte protease granzyme B during apoptosis. *J Biol Chem.* 2000;275(50): 39262-39266.
29. Sutton VR, Vaux DL, Trapani JA. Bcl-2 prevents apoptosis induced by perforin and granzyme B, but not that mediated by whole cytotoxic lymphocytes. *J Immunol.* 1997;158(12): 5783-5790.
30. Maul-Pavicic A, Chiang SCC, Rensing-Ehl A, et al. ORAI1-mediated calcium influx is required for human cytotoxic lymphocyte degranulation and target cell lysis. *Proc Natl Acad Sci USA.* 2011;108(8):3324-3329.
31. Idone V, Tam C, Goss JW, et al. Repair of injured plasma membrane by rapid Ca2+-dependent endocytosis. *J Cell Biol.* 2008;180(5):905-914.
32. Gruenberg J, Maxfield FR. Membrane transport in the endocytic pathway. *Curr Opin Cell Biol.* 1995; 7(4):552-563.
33. Voskoboinik I, Thia M-C, Fletcher J, et al. Calcium-dependent plasma membrane binding and cell lysis by perforin are mediated through its C2 domain: A critical role for aspartate residues 429, 435, 483, and 485 but not 491. *J Biol Chem.* 2005;280(9):8426-8434.
34. Praper T, Besenicar MP, Istinic H, et al. Human perforin permeabilizing activity, but not binding to lipid membranes, is affected by pH. *Mol Immunol.* 2010;47(15):2492-2504.
35. Phillips K, de la Peña AH. The combined use of the Thermofluor assay and ThermoQ analytical software for the determination of protein stability and buffer optimization as an aid in protein crystallization. *Curr Protoc Mol Biol.* 2011;94: 10.28.1-10.28.15.
36. Forgac M. Vacuolar ATPases: rotary proton pumps in physiology and pathophysiology. *Nat Rev Mol Cell Biol.* 2007;8(11):917-929.
37. Kawasaki Y, Saito T, Shirota-Someya Y, et al. Cell death-associated translocation of plasma membrane components induced by CTL. *J Immunol.* 2000;164(9):4641-4648.
38. Walev I, Bhakdi SC, Hofmann F, et al. Delivery of proteins into living cells by reversible membrane permeabilization with streptolysin-O. *Proc Natl Acad Sci USA.* 2001;98(6):3185-3190.
39. Reddy A, Caler EV, Andrews NW. Plasma membrane repair is mediated by Ca(2+)-regulated exocytosis of lysosomes. *Cell.* 2001;106(2):157-169.
40. Trapani JA, Jans DA, Jans PJ, et al. Efficient nuclear targeting of granzyme B and the nuclear consequences of apoptosis induced by granzyme B and perforin are caspase-dependent, but cell death is caspase-independent. *J Biol Chem.* 1998;273(43):27934-27938.
41. Trapani JA, Jans P, Smyth MJ, et al. Perforin-dependent nuclear entry of granzyme B precedes apoptosis, and is not a consequence of nuclear membrane dysfunction. *Cell Death Differ.* 1998; 5(6):488-496.
42. Trapani JA, Sutton VR, Thia KYT, et al. A clathrin/dynamin- and mannose-6-phosphate receptor-independent pathway for granzyme B-induced cell death. *J Cell Biol.* 2003;160(2):223-233.
43. Gerasimenko JV, Tepikin AV, Petersen OH, et al. Calcium uptake via endocytosis with rapid release from acidifying endosomes. *Curr Biol.* 1998;8(24): 1335-1338.